

# Mass distributions for quasifission processes in superheavy composite systems with $Z=108-120$

G.N. Knyazheva, A.A. Bogachev, I.M. Itkis, M.G. Itkis, E.M. Kozulin

FLNR, Joint Institute for Nuclear Research, 141980 Dubna, Russia

**Abstract.** This paper presents the study of mass-energy distributions of quasifission fragments obtained in the reactions  $^{36}\text{S}$ ,  $^{48}\text{Ca}$ ,  $^{64}\text{Ni}+^{238}\text{U}$  at energies below and above the Coulomb barrier. To describe the quasifission mass distribution the simple model has been proposed. This model is based on the driving potential of the system and time dependent mass drift. This procedure allows to estimate QF time scale from the measured mass distributions.

## 1 Fission and quasifission processes

In the reactions with heavy ions complete fusion and quasifission (QF) are competing processes. The relative contribution of QF to the capture cross section becomes dominant for superheavy composite systems and compound nucleus (CN) formation is hindered by the QF process. The balance between the two processes strongly depends on the entrance channel properties.

The QF is characterized by significant nucleon exchange and energy dissipation [1, 2] and QF fragments exhibit similar characteristics to fragments of CN-fission process; therefore, distinguishing between CN-fission and QF fragments is complicated, especially for symmetric mass split.

It is known that in superheavy composite systems QF leads to the formation of the asymmetric fragments with mass asymmetry  $\sim 0.4$  [3]. This type of QF process, so-called asymmetric quasifission, is characterized by asymmetric angular distributions in the centre-of-mass system and thus fast reaction times ( $10^{-21}\text{s}=1\text{zs}$ ) [1, 2]. Besides the asymmetric also the symmetric component may be affected by the presence of the QF process. The angular distribution is symmetric for this type of QF that is similar to CN-fission. But in the case of QF, the anomalously large fragment anisotropies relative to those expected from CN-fission have been observed [4].

Despite the fact that QF was discovered about 30 year ago, and a lot of studies on mass and angular distributions for different reactions have been done, at present there is no data on systematic behaviour of the properties of QF fragments, such as mass distribution, its dispersion, TKE, in dependence on incident energy, since in previous investigations the main attention was paid to fusion probabilities and fusion-fission properties and QF has been considered as interfered process mainly.

<sup>a</sup> Corresponding author: knyazheva@nr.jinr.ru

## 2 Mass-energy distributions for the $^{36}\text{S}$ , $^{48}\text{Ca}$ and $^{64}\text{Ni}$ ions with $^{238}\text{U}$

Fig. 1 shows the mass-energy distributions of binary fragments obtained in the reactions of  $^{16}\text{S}$ ,  $^{48}\text{Ca}$ ,  $^{64}\text{Ni}$  ions with uranium target at energies close to the Coulomb barrier. These data have been measured by two time-of-flight CORSET spectrometer [5, 6]. The mass resolution of the spectrometer for these measurements was about 3u (FWHM) that allows to investigate the features of mass distributions with good accuracy. The Coulomb factors are strongly different for these systems: from 1472, 1840 to 2576 for the  $^{16}\text{S}+^{238}\text{U}$ ,  $^{48}\text{Ca}+^{238}\text{U}$  and  $^{64}\text{Ni}+^{238}\text{U}$ , respectively. Mass-energy distributions of all studied systems have typical wide two-humped shape caused by QF under the influence of closed shells with  $Z=82$  and  $N=50, 126$ . Generally, in heavy-ion-induced reactions the formation of  $\text{QF}_{\text{asym}}$  fragments is connected with strong influence of the nuclear shell with  $Z=82$  and  $N=126$  (doubly magic lead). In fact, as was shown in Ref. [5], for the  $^{48}\text{Ca}+^{238}\text{U}$  reaction the maximum yield corresponds to fragments with masses 208 u. However, in reactions with lighter projectiles on a uranium target, the asymmetric QF peak shifts towards more symmetric masses [6]. By contrast, for the heavier projectile  $^{64}\text{Ni}$ , the maximum yield of  $\text{QF}_{\text{asym}}$  fragments corresponds to the heavy mass 215 u [5]. In the bottom panel of Fig. 1 the driving potentials at scission point calculated with NRV code [7] using the proximity model together with experimental mass distributions are shown. It is clearly seen that the minimum of the driving potential corresponds to the maximum of the yield of asymmetric QF fragments. So, while the relative contribution of QF to the capture cross section mainly depends on the

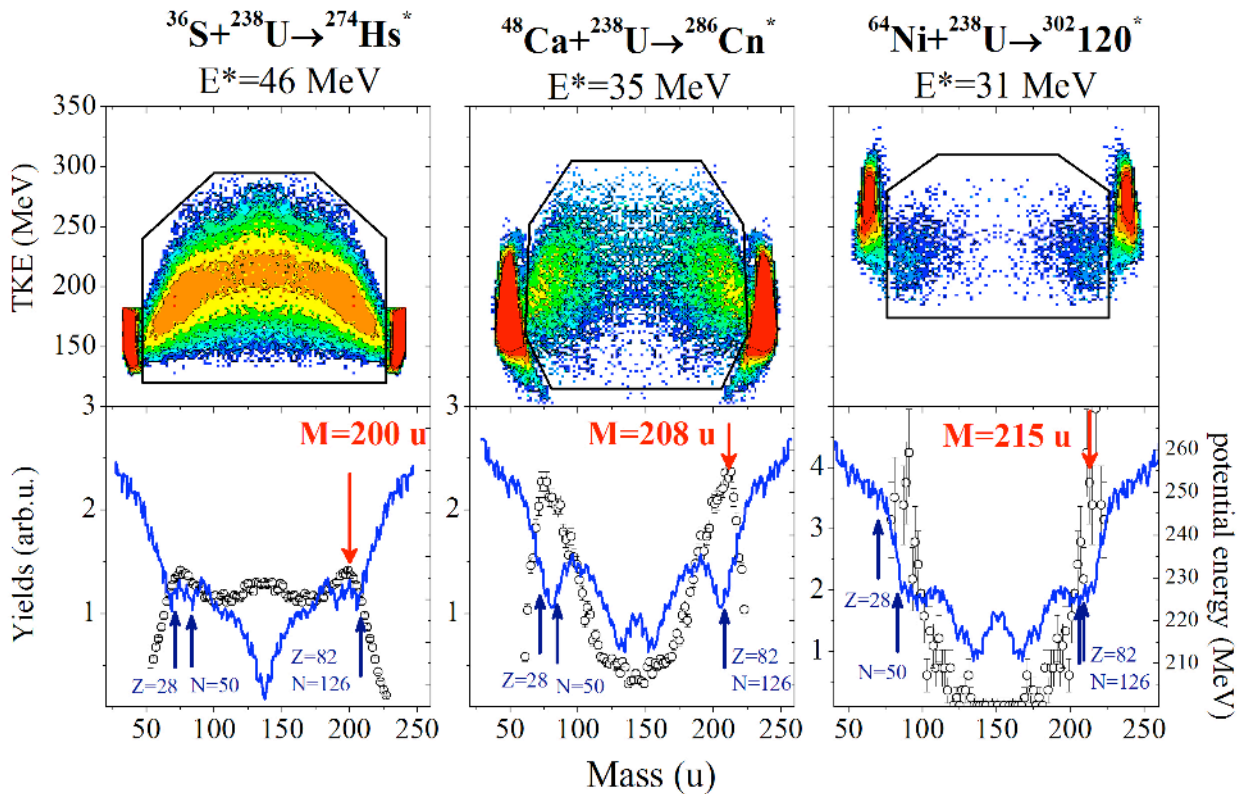


**Figure 1.** Top: Mass-energy distributions for the reactions  $^{36}\text{S} + ^{238}\text{U} \rightarrow ^{274}\text{Hs}^*$ ,  $^{48}\text{Ca} + ^{238}\text{U} \rightarrow ^{286}\text{Cn}^*$ ,  $^{64}\text{Ni} + ^{238}\text{U} \rightarrow ^{302}\text{120}^*$  at energies close to the Coulomb barrier; bottom: open circles are mass distributions for fission-like fragments inside the contour line on M-TKE matrices and solid lines are the driving potentials as a function of mass for studied systems.

reaction entrance channel properties, the features of asymmetric QF are essentially determined by the driving potential of a composite system.

### 3 Mass-angular distributions: time for the asymmetric QF process

In the reactions with  $^{238}\text{U}$ -ions [1] the mass energy and angular distributions of QF fragments have been measured and the time scale for mass transfer in QF reactions has been derived from turning angles of the composite system. It has been found that the mass drift towards symmetry shows the characteristics of an overdamped motion with a universal time constant independent on scattering system and bombarding energy. It indicated that the drift forward mass symmetry occurs as overdamped motion given by:

$$\frac{\Delta A}{\Delta A_{\max}} = \frac{A_t - \langle A \rangle}{\frac{1}{2}(A_t - A_p)} = 1 - \exp[-(t - t_0)/\tau] \quad (1)$$

where  $\tau = (5.3 \pm 1) \text{zs}$  is the time constant common to all systems,  $t_0 - 1 \text{zs}$  is a time delay before mass drift sets in,  $A_t$  and  $A_p$  are the mass of target and projectile, respectively. The uncertainties in Eq. 1 are connected mainly with the calculation of moments of inertia for dinuclear systems. It follows from the equation that the key ingredient for the mass transfer is the distribution of the interaction time of the system.

Recently, the QF time scale has been derived from the measurements of mass-angular distributions for the reactions  $^{186}\text{W} + ^{34}\text{S}$ ,  $^{48}\text{Ti}$  and  $^{64}\text{Ni}$  [8]. In this work the QF time distributions were parameterized using a half Gaussian followed by an exponential decay. The average ( $\tau_0$ ) and width of the Gaussian, and the decay time ( $\tau_1$ ), were individually adjusted to reproduce the measured mass-angular distributions.

### 4 The degree of mass drift as a tool to extract time scale for the asymmetric QF process

Using the assumption for time distribution for QF process proposed in Ref. [8] together with the Eq. 1 it is possible to calculate the mass distribution for QF fragments. But, in the previous section it was shown that QF fragments are affected strongly by the shell effects. So, taken into account the shell effects in QF process, in the first approximation, the yield of QF fragment mass can be written as:

$$Y_{\text{QF}}(A) = p(U(A)) \cdot p(A(t)) \quad (2)$$

where  $p(U(A))$  is the probability connected with the driving potential of the system (minimum of the driving potential corresponds to  $p(U(A))=1$  and value of driving potential for the entrance channel corresponds to  $p(U(A))=0$ ). The driving potentials were calculated as a sum of the LDM potential at distance of 15 fm between

the mass centers of dinuclear system calculated with NRV code [7] and shell correction in ground state taken from [9]. It should be noted that the proximity model gives a very similar potential. The term  $p(A(t))$  in Eq. 2 is the probability to exchange number of nucleons of  $\Delta A = A_r - A$  at given fragment mass  $A$  and time  $t$  calculated with Eq. (1) in the assumption of the time distribution for QF from Ref. [6]. We have adjusted the parameters  $\tau_0$  and  $\tau_1$  (average of the Gaussian and decay time) of the QF time distribution to obtain the best agreement between experimental and calculated with Eq. 2 mass distributions. This procedure gives the possibility to extract the QF time scale from measured mass distributions with the accuracy of about 20% (mainly determined by the mass resolution of the experimental spectra).

When nuclei come to contact in the reactions with heavy ions they become excited, and fluctuations play an important role in the further evolution of the compound system. Due to these fluctuations fragments formed in the QF<sub>asym</sub> process could have masses close to symmetry with some probability. To take into account these possible fluctuations in the present analysis the yield of obtained with Eq. 2 mass distribution was spread by Gaussian distribution for each fragment mass. The value of sigma of the Gaussian distribution was chosen the same for all masses and was obtained from the fitting procedure of the experimental mass distribution by the Eq. 2. It results in 13 u at energies above the barrier and monotonically decreases up to 2 u for energy  $E_{c.m.}/E_B = 0.94$ .

Figures 2-4 show the calculated mass distribution for QF process using the proposed method in comparison with the experimental mass distribution of fission-like fragments for the reactions of  $^{238}\text{U}$  with  $^{36}\text{S}$ ,  $^{48}\text{Ca}$  and  $^{64}\text{Ni}$  ions at energies below and above the Bass barrier. In the fitting procedure with Eq. 2 the values of  $\tau_0$  and  $\tau_1$  is determined by the outside and inside shape of asymmetric QF mass distribution respectively. The width of the experimental QF<sub>asym</sub> distributions increases with increasing collision energies for the all studied reactions. For the case of the  $^{36}\text{S}$  reaction decomposition into compound nucleus fission and QF obtained from the analysis of the total kinetic energy distributions of fission-like fragments (see Ref. [6] for details of this procedure) is also presented in Fig. 2. It is clearly seen that proposed method to describe the QF mass distribution gives good agreement with experimental data at energies above the barrier. At energies below the barrier the contribution of symmetric fragments formed in QF process estimated using this method is rather smaller than that obtained from the analysis of the TKE distribution. If one assumes that fluctuation of mass in QF process (sigma) is not constant for all fragment masses and dependent on the second derivative of the potential energy surface for given fragment mass, it is possible to reproduce the symmetric part at energies below the barrier. But in this case the number of variable parameters increases and more experimental data are needed for reasonable choice of the parameters.

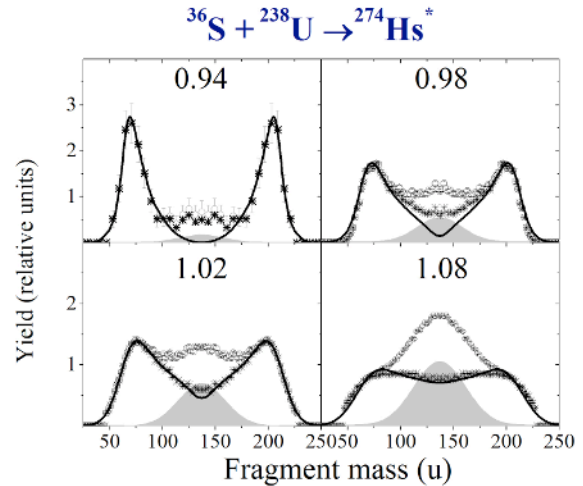


**Figure 2.** Mass distributions of fission-like fragments for the reaction  $^{36}\text{S} + ^{238}\text{U} \rightarrow ^{274}\text{Hs}^*$  at different energies ( $E_{c.m.}/E_B$  is indicated for each plot); the filled regions and stars are the contribution of CN-fission and QF obtained from the analysis of TKE (see Ref.[6] for details), the lines are the fits of the experimental data with using Eq. 2.

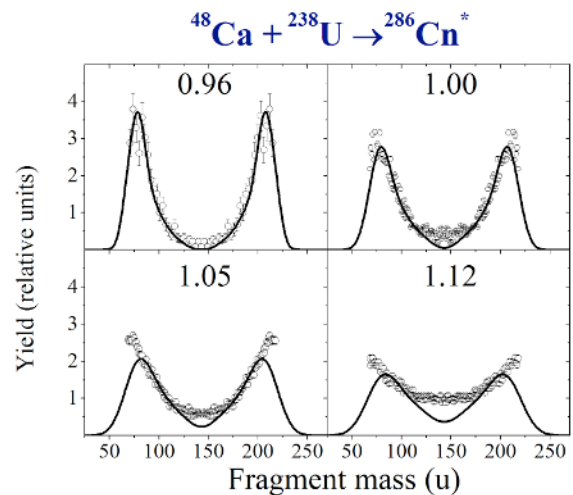


**Figure 3.** The same as Fig. 2 but for the reaction  $^{48}\text{Ca} + ^{238}\text{U}$ .

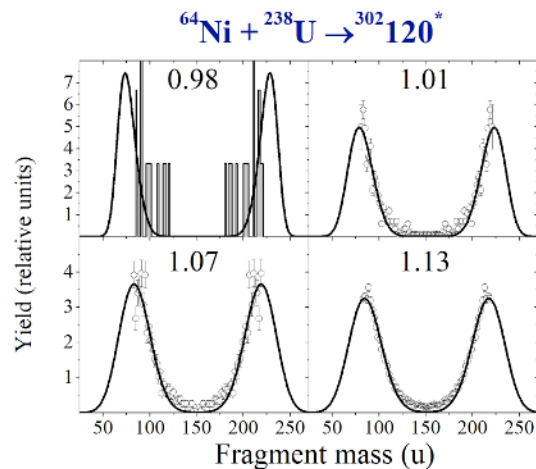


**Figure 4.** The same as Fig. 2 but for the reaction  $^{64}\text{Ni} + ^{238}\text{U}$ .

As it was mentioned above, we supposed that the fluctuation ( $\sigma$ ) is constant for all fragment masses and depends only on the collision energy.

In the case of  $^{48}\text{Ca}$  beam the events of quasi-elastic and deep-inelastic scattering are overlapped with QF fragments, especially at energies above the barrier. Due to this reason in this reaction for fragments close to projectile and target masses the experimental yield is larger than it was predicted at energies above the barrier. In the symmetric mass region the calculated yields for QF are smaller than the experimental ones for all measured energies. It should be connected with contribution of fusion-fission process. The analysis of the TKE for symmetric fragments formed in the reaction  $^{48}\text{Ca}+^{238}\text{U}$  made in Ref. [5] showed the presence of the component with the features appropriate to fusion-fission process.

In the case of the reaction with  $^{64}\text{Ni}$  ions asymmetric fragments with masses close to projectile and target were not detected due to the choice of the angular position of the CORSET spectrometer arms [5]. The mass-energy distribution of binary fragments obtained in the reaction  $^{64}\text{Ni}+^{238}\text{U}$  is shown in Fig. 5. On this figure the grey region indicates the fragments with given mass and TKE for which the detection efficiency is zero due to the reaction kinematics and finite size of the spectrometer arms. In this measurement the time-of-flight arms of the spectrometer have been installed at angles the most suitable for maximum yield of symmetric fragments. Therefore, the experimental mass distributions for fission-like fragments for the reaction  $^{64}\text{Ni}+^{238}\text{U}$  start from the mass about 80 u. This factor has been taken into account in fitting procedure with Eq. 2 and the calculated curves overstep the experimental distributions. As in the case of  $^{48}\text{Ca}$  reaction the calculated yields of symmetric fragments are smaller than experimental ones, but the analysis of the TKE distributions for these symmetric fragments (see Ref. [5]) showed that it should be connected with symmetric QF process.

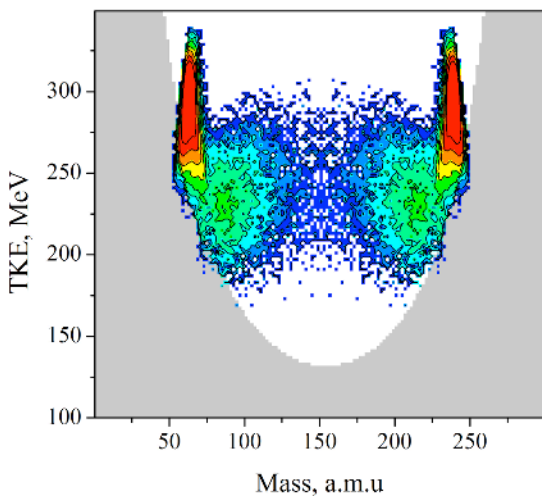


**Figure 5.** Mass-energy distribution of binary reaction fragments obtained in the reaction  $^{64}\text{Ni}+^{238}\text{U}$  at  $E_{\text{lab}}=382\text{MeV}$ . The grey region indicates the area with zero efficiency of coincident fragments.

Nevertheless, the method describes well the asymmetric QF mass distribution and may be applied for

estimation of the time scale for the asymmetric QF process. The obtained average time ( $\tau_0+\tau_1$ ) from this fitting procedure as a function of energy above the Bass barrier is shown in Fig. 6 for the reactions  $^{36}\text{S}$ ,  $^{48}\text{Ca}$ ,  $^{64}\text{Ni}+^{238}\text{U}$ .

The strong decreasing of the QF has been observed at the transition from  $^{36}\text{S}$  to  $^{64}\text{Ni}$  ions. At barrier energy the time scale for QF in the reaction with  $^{36}\text{S}$  is about 6zs,  $^{48}\text{Ca}$  – about 3zs and  $^{64}\text{Ni}$  – 0.5zs.

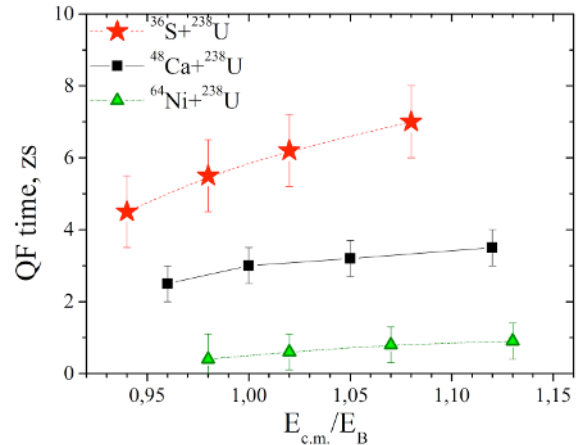


**Figure 6.** The derived time scales for asymmetric QF process for the reactions of  $^{238}\text{U}$  with  $^{36}\text{S}$ ,  $^{48}\text{Ca}$  and  $^{64}\text{Ni}$  beams.

In summary, from the analysis of mass-energy distributions of fission-like fragments formed in the reactions  $^{36}\text{S}$ ,  $^{48}\text{Ca}$ ,  $^{64}\text{Ni}+^{238}\text{U}$  it was found:

1. While the relative contribution of QF to the capture cross section mainly depends on the reaction entrance channel properties, the features of asymmetric QF are determined essentially by the driving potential of a composite system.
2. The drift to the symmetry in the QF mass distributions increases with increasing of the projectile energy.
3. The interaction time for asymmetric QF process decreases with increasing the Coulomb factor  $Z_1Z_2$ .

This work was supported by the Russian Foundation for Basic Research (Grant No. 13-02-01282-a) and the JINR Grant No. 13-501-03.

## References

1. W.Q. Shen et al., Phys. Rev. C **36**, 115 (1987)
2. R. Bock et al., Nucl. Phys. A **388**, 334 (1982)
3. M.G. Itkis et al., Nucl. Phys. A **787**, 150c (2007).
4. B.B. Back, Phys. Rev. C **31**, 2104 (1985)
5. E.M. Kozulin et al, Phys. Lett. B **686**, 227 (2010)
6. I.M. Itkis et al., Phys Rev. C (2011)
7. V.I. Zagrebaev et al., nrv.jinr.ru
8. R. Du Rietz et al., Phys. Rev. Lett **106**, 052701 (2011)
9. P. Moller, J.R. Nix, W.D. Myers, W.J. Swiatecki, At. Data Nucl. Data Tables **59**, 185 (1995)